Clays and Clay Minerals, Vol. 69, No. 6:663–671, 2021

A COMPARISON OF THE ADSORPTION OF CESIUM ON ZEOLITE MINERALS VS VERMICULITE

D. R. Ferreira[1]*, G. D. Phillips[2], and B. Baruah[2]

[1]Department of Ecology, Evolution, and Organismal Biology, Kennesaw State University, 370 Paulding AvenueGA 30144 Kennesaw, USA

[2]Department of Chemistry and Biochemistry, Kennesaw State University, 370 Paulding Avenue, Kennesaw, GA 30144, USA

Abstract—Radiocesium was deposited on the soils of Fukushima Prefecture in Japan after the meltdown of the Fukushima Daiichi Nuclear Power Plant in 2011. The radiocesium bound to 2:1 clay minerals, such as vermiculite, common in the soil of that region and became non-exchangeable due to the strong affinity of these clay minerals for the Cs^+ adsorbed. The current study generated adsorption envelopes for Cs^+ on three zeolite minerals: zeolite Y, ZSM-5, and ferrierite. Two of these (ZSM-5 and ferrierite) caused monovalent cations to adsorb via a strong inner-sphere mechanism. A comparison of Cs^+ adsorption on these zeolites to Na^+ adsorption on the same zeolites showed that Cs^+ adsorbs much more strongly than Na^+, which is explained by its atomic properties. Despite the inner-sphere adsorption of Cs^+ on ZSM-5 and ferrierite, the affinity of vermiculite for Cs^+ is even stronger. An adsorption envelope for Cs^+ on vermiculite failed to show a low-pH adsorption edge even at a pH of 1.01, with adsorption remaining at ~65% of the maximum even at this low pH. The adsorption envelopes for Cs^+ on ZSM-5 and ferrierite minerals did show low-pH adsorption edges centered at pH 3.5 and 3.0, respectively, where Cs^+ adsorption dropped to zero. The greater affinity of vermiculite for Cs^+, even when compared with that for two zeolite minerals known to have significant affinities for monovalent ions, highlights the difficulty in removing Cs^+ from contaminated Fukushima soils.

Keywords—Adsorption · Cesium · Vermiculite · Zeolite

INTRODUCTION

Cs^+ is relatively rare in natural systems, especially in the soil environment (Groenewold et al., 1998). Since the Tohoku Earthquake of 2011, the subsequent meltdown of the Fukushima Daiichi Nuclear Power Plant, and the introduction of radioactive ^{133}Cs and ^{137}Cs (radiocesium) to surface soils in Fukushima Prefecture in Japan (Weiss & Bourgeois, 2012), there has been increased interest in a better understanding of the behavior of Cs^+. A recent report (Fuji et al., 2014) demonstrated that 2:1 clays such as vermiculite and other similarly structured minerals have an unusually high affinity toward Cs^+. That affinity is largely responsible for the sequestration of radiocesium in the top 5 cm of the surface soil (Tanaka et al., 2012). When Cs^+ is adsorbed in the interlayer space of 2:1 clays such as vermiculite, the Cs^+ can collapse the interlayer space of those clays and become non-exchangeable. The trapped radiocesium in the collapsed interlayer space cannot be removed chemically without dissolving the mineral structure (Sawhney, 1964, 1972; Lomenick & Tamura, 1965; Comans & Hockley, 1992; Missana et al., 2004; Iijima et al., 2010; Kogure et al., 2012; Dzene et al., 2015; Fuller et al., 2015). Given these issues, an improvement in our understanding of the interaction between radiocesium and vermiculite in those soils is vitally important.

The mechanism of irreversible Cs^+ adsorption on vermiculite and other similar 2:1 clays in Japanese surface soils is very similar to the irreversible adsorption of potassium ions (K^+) on micas, about which much research has been published (Gaines Jr., 1957; Dolcater et al., 1972; Perkins & Tan, 1973; Sparks et al., 1980; Martin & Sparks, 1985; Sparks & Carski, 1985; Sparks, 1987; Pal & Durge, 1989; Osman et al., 1998, 1999). The adsorption of Cs^+ on vermiculite and other similar 2:1 clays has been explored to a lesser extent, however. When K^+ is adsorbed in the interlayer space of 2:1 clay minerals, it prompts the collapse of the interlayer space, trapping the K^+ inside and rendering the K^+ non-exchangeable. The surfaces of the tetrahedral sheets of these clay minerals contain numerous ditrigonal siloxane cavities. These cavities form due to the inability of the electron clouds of adjacent oxygen atoms to overlap at the base where the two neighboring silica tetrahedra meet. The Cs^+ radius is ~1.8 Å, which is close to the size of the ditrigonal siloxane cavity, 2.6 Å (Sato et al., 2013). Thus, Cs^+ fits into the cavity tightly, with one cavity encapsulating the top half of the Cs^+ and another cavity encapsulating the bottom half of the Cs^+(Fig. 1). This tight fit prompts the cesium ions to adsorb inside the interlayer spaces of certain 2:1 clay minerals such as vermiculite using a robust inner-sphere mechanism (Bostick et al., 2002; Okumura et al., 2013). Once the inner-sphere adsorption prompts the interlayer to collapse, the ions can act as a glue and seal the interlayer shut, preventing re-expansion and trapping the adsorbed ions inside. Research has shown that Cs^+ can collapse clay interlayers in the same way and seal the interlayer even more tightly, causing the trapped Cs^+ to become even more challenging to desorb than K^+(Coleman et al., 1963).

A recent study examining the interaction between Cs^+ on vermiculite elucidated a very unusual phenomenon when adsorption envelopes for Cs^+ on vermiculite were generated

* E-mail address of corresponding author: dferreira@kennesaw.edu

DOI: 10.1007/s42860-021-00150-9

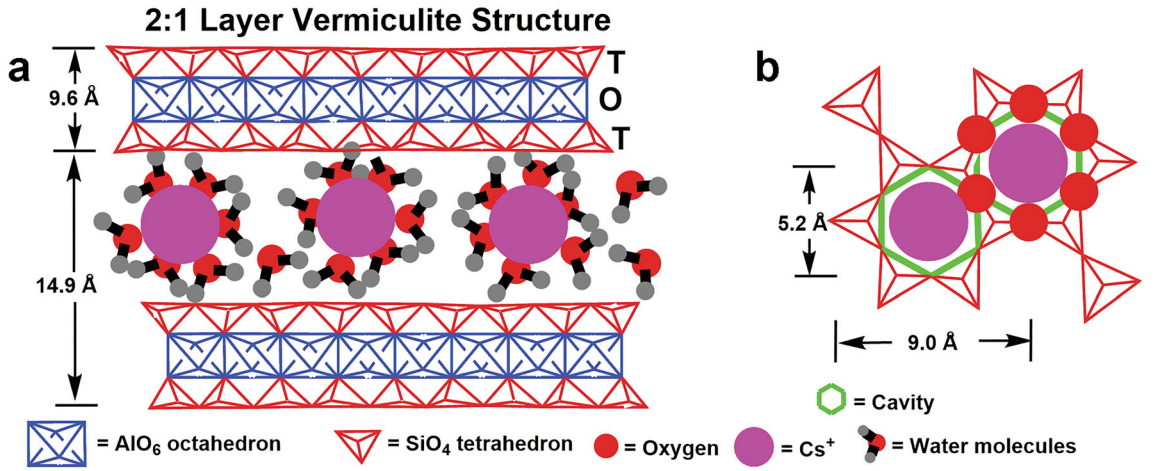

Fig. 1. Schematic representation of Cs^+ being adsorbed on vermiculite: **a** side view of Cs^+ dehydrating as it moves from the bulk solution to adsorb in the vermiculite interlayer space and collapse it; and **b** top view of one ditrigonal siloxane cavity with Cs^+ ion surrounded by O atoms of the tetrahedral sheet (Huang et al., 2017; Yamamoto et al., 2019)

(Ferreira et al., 2018). Adsorption envelopes have long been used to compare the adsorption of different ions on the same mineral and to compare the affinity of different minerals for particular ions (Cabrera et al., 1977; McKenzie, 1983; Sposito et al., 1988; Schulthess & Huang, 1991; Manning & Goldberg, 1996; Raven et al., 1998; Arai & Sparks, 2001; Lafferty & Loeppert, 2005; Schulthess et al., 2011; Ferreira & Schulthess, 2011). Adsorption edges, which are revealed by adsorption envelopes, can be used to understand the strength with which a particular ion adsorbs on the surface of a mineral. The adsorption edge is where the amount of the ion adsorbing changes dramatically over a relatively small pH range. Adsorption edges are characterized by a sharp vertical drop in the adsorbing ion concentration (*y*-axis) as the pH (*x*-axis) decreases. Adsorption edges represent a pH range where the increasing concentration of H^+ (decreasing pH) increases the competitiveness of H^+ for adsorption sites, allowing H^+ to prevent the ion of interest from adsorbing on a particular surface. Typically, the lower the pH at which these adsorption edges occur, the stronger the adsorption of the ion on that particular mineral is considered to be; a greater concentration of H^+ is required to prevent the ion from adsorbing.

For the adsorption envelope of Cs^+ on vermiculite (Ferreira et al., 2018), a pH as low as 1.01 failed to elucidate an adsorption edge that would reduce the adsorption of Cs^+ to zero. In fact, at a pH of 1.01, the amount of Cs^+ being adsorbed was decreased by only 35% from its maximum at pH 8.39. Increasing the concentration of H^+ in the system by more than seven orders of magnitude was able to decrease the amount of Cs^+ being adsorbed by only 35%. Even at a concentration of 0.1 M, the H^+ was unable to reduce the adsorption of Cs^+, which was present at a concentration of only 0.02 M, to zero. This unusual occurrence raises the question of whether this phenomenon is unique to Cs^+ adsorption on vermiculite or whether other minerals that are known to adsorb monovalent ions strongly would also demonstrate this sort of behavior. This could be addressed through a study of adsorption envelopes for cesium on other minerals known to adsorb monovalent ions strongly to determine whether the behavior of cesium on vermiculite is, in fact, unique to vermiculite.

An exploration of the Nanopore Inner-Sphere Enhancement (NISE) effect has shown that ions which typically adsorb weakly on external surfaces, such as monovalent ions, can be bound tightly to mineral surfaces through inner-sphere adsorption mechanisms when placed into confining environments such as the nanoporous channels of zeolite minerals (Ferreira & Schulthess, 2011; Ferreira et al., 2012, 2013). Zeolites are aluminosilicate minerals with crystalline structures that create nanopore channels. Zeolite minerals, of which 241 are known to exist, each has its own unique structure and nanoporosity (Baerlocher & McCusker, 2020), of which 50 are natural (Flanagan & Crangle Jr, 2017) and 191 are synthetic. Due to their very large surface area, zeolites can be used as catalysts in chemical reactions such as petroleum refining, as separation membranes, or as photochemical hosts (Song et al., 2004). Their nanoporosity also makes them interesting substrates for the study of the adsorption of ions. The NISE effect may explain the strong adsorption of monovalent ions such as K^+ and Cs^+ in a confining environment such as a collapsed 2:1 clay interlayer, which can reach the dimensions comparable to zeolite nanopores or even smaller. Recent research into the adsorption of Cs^+ on vermiculite showed that the interlayer of vermiculite collapses to a dimension of 0.12 nm (Ferreira et al., 2018), which is small enough to trigger the NISE effect and prompt strong inner-sphere adsorption of monovalent cations. If the unusually strong adsorption of cesium on vermiculite is, in fact, due to the small size of the interlayer dimension after it collapses, that behavior should also occur on zeolite minerals with small nanopore dimensions that would trigger the NISE Effect. The objective of the current study, therefore, was to determine whether the adsorption envelopes for cesium on zeolite minerals would mimic the behavior that was observed for cesium on vermiculite.

https://doi.org/10.1007/s42860-021-00150-9 Published online by Cambridge University Press

MATERIALS AND METHODS

The zeolite minerals used in the present study were purchased from Zeolyst International (Conshohocken, Pennsylvania, USA). Their nanopore dimensions and chemical properties are listed in Table 2. The nanopores in these zeolites are interconnected, allowing for free movement of ions within the interior of the minerals. Zeolite Y (CBV901) [$(NH_4)_{3.5}[Al_7Si_{17}O_{48}]\cdot 32(H_2O)$] was purchased as a hydrogen-form, meaning that its surfaces had only H^+ adsorbed. ZSM-5(CBV8014) [$H_nAl_nSi_{96-n}O_{192}\cdot 16H_2O$ ($0<n<27$)] and ferrierite (CP914C) [$(NH_4)(Si,Al)_{18}O_{36}\cdot 9(H_2O)$] were purchased as ammonium forms and were converted into H forms by placing them in a muffle furnace at 550°C for >18 h, allowing the NH_4 adsorbed to volatilize as NH_3 gas, leaving an adsorbed H^+ behind. This method has been used successfully to convert NH_4-forms to H-forms in previous studies (Ferreira & Schulthess, 2011). The stability of these zeolites at low pH values has also been determined in previous studies. Analyses of Si concentrations in supernatant solutions from zeolites exposed to highly acidic solutions showed dissolution of 0.22% for zeolite Y at pH 1.10, 0.12% dissolution of ZSM-5 at pH 1.61, and 0.05% dissolution of ferrierite at pH 1.06 (Ferreira & Schulthess, 2011). Analyses of Al concentrations in these solutions were below the detection limits of the instrument in most cases; dissolution was calculated based on the Si concentration, therefore, which provided measurable results for all samples. Thus, the decrease in adsorption of Cs^+ for these zeolites at low pH in this study are due to desorption by competing H^+ ions (the only other cation in the system) and not due to dissolution of the mineral.

Adsorption experiments were carried out in 50-mL nominal Oak Ridge centrifuge tubes. Approximately 0.5030 g of zeolite solid (± 0.0030 g) at room temperature and humidity were added to each centrifuge tube along with 7.000 mL of 0.1 M CsOH for a concentration of 20 mM Cs^+. This brought the pH of all samples to the maximum pH values (ranging from 9.64 to 11.36). Varying amounts of 1.21 M HCl were then added to bring the pH of the samples down to allow measurement of the adsorption of Cs^+ at various pH values. An amount of deionized water was then added to bring the total volume of each centrifuge tube to 35.000 mL. Centrifuge tubes were allowed to equilibrate on a hematology mixer for >18 h, ensuring that the environment reached an equilibrium condition. After equilibrating, the centrifuge tubes were centrifuged for 10 min at 7800×*g* to separate the solid and liquid phases. An aliquot of the supernatant was extracted and set aside for pH measurement. Another aliquot was set aside for $[Cs^+]$ measurement. For ion-exchange experiments with Mg^{2+} and Ca^{2+}, the experiments were carried out as described above except that either 10 mM Mg^{2+} or 10 mM Ca^{2+} was added to each centrifuge tube to act as a competitor for the 20 mM Cs^+. The results of the ion-exchange experiment are based on three samples of each zeolite equilibrated with Cs^+ and Mg^{2+} and three samples of each zeolite equilibrated with Cs^+ and Ca^{2+}. A small amount of acid was added to each of the centrifuge tubes for the ion-exchange experiment in order to prevent any possible precipitation of the divalent ions.

Cesium concentrations were determined via ICP-OES spectroscopy using a Perkin Elmer (Waltham, Massachusetts, USA) Avio 200 instrument. Cesium was measured using a wavelength of 894.353 nm with an axial view. Quality control procedures for the analysis were used every 10 samples to ensure that the calibration curve was still accurate. Calibration solutions were analyzed as samples and analysis was allowed to continue only if the calculated value for the calibration solution was within ±5% of the original value used to generate the calibration curve. Values for all measurements were calculated as the average of the light intensity for five replicate measurements of each sample.

For each set of samples prepared, one blank was created with the same amount of CsOH but without any zeolite solid added. The concentration of Cs^+ in this blank was recorded as the initial $[Cs^+]$ added. The $[Cs^+]$ remaining in the supernatant of each sample was considered to be the final concentration of Cs^+ in the system after adsorption of Cs^+ onto the zeolite mineral. The amount of Cs^+ adsorbed was then calculated per the following equation: $[Cs^+]_{ads} = [Cs^+]_{initial} - [Cs^+]_{final}$.

Adsorption envelopes were generated by plotting the $[Cs^+]_{ads}$ for each zeolite as a function of pH. An adsorption model was created to fit the data for each zeolite using *IExFit* software version 3.3, distributed by Alfisol.com (Coventry, Connecticut, USA). The model parameters are given in Table 1. The parameter Γ_{max} represents the maximum adsorption capacity of each adsorption site. Goodness of fit of the model for the adsorption data was determined by calculating Efron's pseudo R^2 value using the following equation: $R^2 = 1 - [\Sigma_i(y_i - \hat{\pi}_i)^2]/[\Sigma_i(y_i -)^2]$, where $\hat{\pi}_i$ are the model's predicted values. The pseudo R^2 values for each model are also included in Table 1.

RESULTS AND DISCUSSION

When comparing the adsorption envelopes for Cs^+ on the three zeolite minerals to each other, the adsorption envelope

Table 1. Parameters for models of Cs^+ adsorption on the zeolite Y, ZSM-5, and ferrierite

Zeolite Name	Site 1		Site 2		Site 3		Pseudo R^2
	Γ_{max} (μmol/m^2)	pK	Γ_{max} (μmol/m^2)	pK	Γ_{max} (μmol/m^2)	pK	
Zeolite Y	0.3240	2.0	0.5319	3.2	0.8298	5.2	0.9974
ZSM-5	2.316	2.0	1.099	6.7			0.9807
Ferrierite	2.700	1.4	1.220	6.5			0.9506

https://doi.org/10.1007/s42860-021-00150-9 Published online by Cambridge University Press

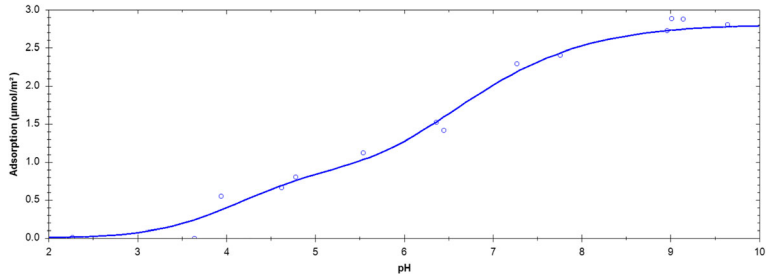

Fig. 2. An adsorption envelope for Cs^+ on zeolite Y. The primary adsorption edge is centered at ~pH 2.5, but has a gentle slope and a low adsorption capacity. A second adsorption edge is centered at ~pH 5, followed by a very slight inflection at ~pH 5.8, followed by a third adsorption edge centered at ~pH 7

for Cs^+ on zeolite Y (Fig. 2) differs in shape and size from the adsorption envelopes for ZSM-5(Fig. 3) and ferrierite (Fig. 4). Characteristics of these zeolites are provided in Table 2. The adsorption edges for Cs^+ on zeolite Y are more gradual than the other two zeolites, and the amount of Cs^+ adsorbing at each site is much smaller. This behavior indicates that Cs^+ is adsorbing more strongly on ZSM-5 (medium pores) and ferrierite (smallest pores) than Cs^+ is on zeolite Y (largest pores), which is the behavior that the NISE effect predicts for monovalent cations. A study of Cs^+ adsorption preferences by different zeolite minerals also found that the two zeolite minerals with the smallest pore dimensions (mordenite and clinoptilolite) adsorbed more Cs^+ than the other two zeolites in the study (zeolite A and zeolite X) (Johan et al., 2015). The same pattern of preferential adsorption of Cs^+ by the zeolite with the smallest pore occurred in a study of Cs^+ adsorption by chabazite vs zeolite A (Mimura & Kanno, 1985); zeolite Rho vs zeolite A and faujasite (Lee et al., 2017); and for chabazite vs heulandite and stilbite (Baek et al., 2018). Research into the NISE effect showed that the adsorption of monovalent cations increases in strength when the environment in which the cation is adsorbing is ~0.5 nm or smaller in diameter (Ferreira & Schulthess, 2011; Ferreira et al., 2012, 2013). This has implications for the strong Cs^+ adsorption in collapsed vermiculite interlayers, because the interlayer space reaches a dimension of <0.5 nm after adsorbed Cs^+ causes it to collapse (Ferreira et al., 2018).

The model used to fit the adsorption data for zeolite Y was a 3-site model, which was needed to support the inflection in the large, gentle adsorption edge between pH 4 and pH 8. While the inflection around pH 5.5 is subtle, a study investigating the adsorption of Co^{2+} on zeolite Y also found three different adsorption sites (Seo et al., 2014). These three sites are the double 6-ring hexagonal prism, the sodalite cavity, and the supercage, for which experimental data on Co^{2+} showed an adsorption capacity ratio of 1:2:3 (Seo et al. 2014). This matches well with the model established for Cs^+ on zeolite Y, which showed Γ_{max} values of 0.3240 µmol/m^2, 0.5319 µmol/m^2, and 0.8298 µmol/m^2 for the three modeled sites. The difference in shape and extent between the adsorption envelope for zeolite Y and the other two zeolites further emphasizes the difference in the adsorption mechanism between the larger-pore zeolite Y, the smaller-pore ZSM-5, and ferrierite.

While the literature also indicates three separate adsorption sites for both ZSM-5 (Rudziński, et al., 1997) and ferrierite (Pulido et al., 2009), the fit of the 2-site adsorption model for the adsorption data on both of these zeolites was excellent. The adsorption sites available within the nanopores are the straight channel, the intersection, and the zigzag/perpendicular

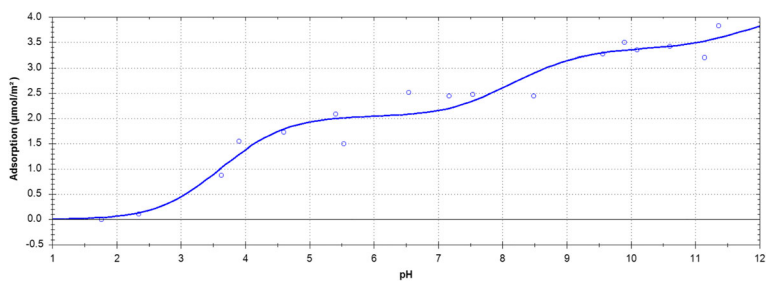

Fig. 3. An adsorption envelope for Cs^+ on ZSM-5. The primary adsorption edge is steep and centered at ~pH 3.5, showing a strong adsorption mechanism for Cs^+ on that surface, which is presumed to be the internal sites within the zeolite nanopores. A second adsorption edge is present, centered at ~pH 8.5, and may represent adsorption of Cs^+ at the intersection of the nanopores

https://doi.org/10.1007/s42860-021-00150-9 Published online by Cambridge University Press

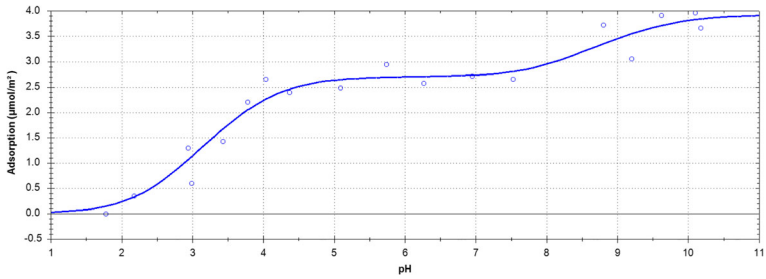

Fig. 4. An adsorption envelope for Cs^+ on ferrierite. The primary adsorption edge is steep and centered at ~pH 3, showing a strong adsorption mechanism for Cs^+ on that surface, which is presumed to be the internal sites within the zeolite nanopores. A second adsorption edge is present, centered at ~pH 9, and may represent adsorption of Cs^+ at the intersection of the nanopores

channel. The adsorption envelope may not have the resolution necessary to distinguish between the adsorption taking place at the three different sites. Indeed, the inflection in the zeolite Y model that necessitated using a third site to fit the data is very subtle. Two of the sites in ZSM-5 and ferrierite, probably the straight and zigzag/perpendicular channels, may have blended together and became indistinguishable in the adsorption envelopes (Figs 3, 4).

The adsorption envelopes for ZSM-5 and ferrierite are remarkably similar in shape to each other. However, they do differ slightly in the pH of the adsorption edges and the height of the central adsorption plateau. While both zeolites have smaller nanopores than does zeolite Y, the nanopores in ferrierite are smaller than those in ZSM-5(Table 2). This may explain the fact that the adsorption envelope for ferrierite has a low-pH adsorption edge occurring at a slightly lower pH than that for ZSM-5 (centered at ~pH 3 vs. ~pH 3.5) and a slightly greater adsorption capacity for its two sites (2.7 µmol/m^2 and 3.9 µmol/m^2) than the two sites for ZSM-5 (2.3 µmol/m^2 and 3.4 µmol/m^2). This difference may also, however, be due to the fact that ferrierite has a lower Si:Al ratio than ZSM-5(Table 2). Other experiments have also noted that ferrierite demonstrated a strong selectivity for Cs^+(Mimura et al., 1992a, 1992b; Seliman, 2012).

To characterize further the strength of the Cs^+ adsorption on these zeolites, an ion-exchange experiment was carried out to determine whether competition with divalent ions Mg^{2+} or Ca^{2+} would affect significantly the amount of Cs^+ being adsorbed. The results of this experiment are presented in Table 3. The addition of Mg^{2+} and Ca^{2+} as ion-exchange competitors for Cs^+ yielded very different results depending on the zeolite in which the competition was taking place. For zeolite Y, which has the largest nanopores, the addition of Mg^{2+} or Ca^{2+} to the system severely decreased the amount of Cs^+ adsorption taking place. However, the Mg^{2+} and Ca^{2+} were both ineffective competitors against Cs^+ for adsorption sites on ZSM-5 and ferrierite, with the amount of Cs^+ adsorbing on those minerals remaining essentially the same despite the addition of the divalent competitors. This is further confirmation of the strong affinity of the two zeolites with smaller nanopores for Cs^+ and matches data collected for competition between Na^+ and Ca^{2+} on these zeolites (Ferreira & Schulthess, 2011). While Mg^{2+} may be small enough to access easily confining environments such as the nanopores of zeolite minerals or the collapsed interlayers of 2:1 clay minerals such as vermiculite, these results cast doubt on the ability of Mg^{2+} to act as an effective ion-exchange agent to remove adsorbed Cs^+ in those environments because the equilibrium appears to favor Cs^+ in such competitions.

Adsorption envelopes for the monovalent ions Na^+ and K^+ on zeolite Y, ZSM-5, and ferrierite showed that both ions adsorbed more weakly on zeolite Y and more strongly on ZSM-5 and ferrierite (Ferreira and Schulthess, 2011). Subsequent NMR analyses of Na^+ on zeolite Y and ZSM-5 confirmed that Na^+ was adsorbing through an outer-sphere mechanism on zeolite Y and through an inner-sphere mechanism on

Table 2. Properties of zeolite minerals. Pore dimensions were taken from the database of zeolite structures (http://www.iza-structure.org/). Surface areas were provided by Zeolyst International (Conshohocken, Pennsylvania, USA)

Zeolite name	Pore dimensions (nm)		Pore-size class	Surface area (m^2 g^{-1})
Zeolite Y	0.74×0.74	N/A*	Largest	700
ZSM-5	0.51×0.55	0.53×0.56	Medium	425
Ferrierite	0.54×0.42	0.48×0.35	Smallest	400

*N/A: not applicable

https://doi.org/10.1007/s42860-021-00150-9 Published online by Cambridge University Press

Table 3. Comparison of Cs^+ adsorption on zeolite Y, ZSM-5, and ferrierite alone vs. in the presence of an equivalent concentration of Mg^{2+} or Ca^{2+} showing that divalent ions are able to reduce Cs^+ adsorption by a sizable amount on zeolite Y, but are ineffective at reducing Cs^+ adsorption in ZSM-5 and ferrierite

Ion Exchange Competition	pH	Cs^+ only adsorbed on zeolite minerals alone (μmol/m^2)	Cs^+ adsorbed on zeolite minerals with competition (μmol/m^2)	Decrease in Cs^+ adsorbed
Zeolite Y (Mg^{2+})	3.64	0.3247	0.2415	25.6%
ZSM-5 (Mg^{2+})	2.63	0.2423	0.2427	–0.2%
Ferrierite (Mg^{2+})	2.13	0.3278	0.3251	0.8%
Zeolite Y (Ca^{2+})	3.73	0.3247	0.1839	43.3%
ZSM-5 (Ca^{2+})	2.66	0.2423	0.2533	–4.5%
Ferrierite (Ca^{2+})	2.16	0.3278	0.3220	1.8%

ZSM-5(Ferreira et al., 2012). This was further confirmed by a calorimetry study of the heat of adsorption on zeolite Y and ZSM-5(Ferreira et al., 2013). The difference in the adsorption mechanism between these zeolites was attributed to the fact that zeolite Y contained nanopore channels with larger dimensions than the nanopore channels of ZSM-5 and ferrierite (Table 2).

Because Cs^+ is also monovalent, it was expected to follow the same pattern of adsorption mechanisms on these zeolites as was demonstrated for Na^+ and K^+. The presence of K^+ decreased significantly Na^+ adsorption on all three zeolites when added as a competitor at an equal concentration (Ferreira & Schulthess, 2011). This was attributed to the fact that K^+ has a considerably larger ionic diameter than Na^+(Table 4). Thus, K^+ could fit more snugly in the nanopore channels of the zeolites, allowing K^+ to adsorb more closely to the mineral surface and form a stronger electrostatic attraction to the adsorption sites available. The fact that K^+ has lower hydration energy than Na^+(Table 4) also means that K^+ can dehydrate in confined environments more easily since its bond with its hydrating water molecules is weaker than the bond between Na^+ and its hydrating water molecules (Teppen & Miller, 2006). This is also reflected in the fact that K^+ has a smaller hydrated diameter than Na^+(Table 4) despite its larger ionic diameter.

Based on the trends established for Na^+ and K^+, it was expected that Cs^+ would adsorb more strongly because Cs^+ has a larger ionic diameter and lower hydration energy than either Na^+ or K^+(Table 4). A recent study investigating the impact of adding K^+ as an ion-exchange competitor for Cs^+ on the 2:1 clay mineral vermiculite showed that K^+ had almost no effect on the ability of Cs^+ to adsorb in vermiculite interlayers (Ferreira et al., 2018). Other studies have also found that K^+ is ineffective in ion-exchange competitions with Cs^+ on vermiculite (Sikalidis et al., 1988; Akalin et al., 2018). These data support further the idea that Cs^+ adsorption in confined environments should be stronger than both Na^+ and K^+. The adsorption envelopes for Cs^+ on zeolite Y, ZSM-5, and ferrierite (Figs 2–4) did indeed confirm this hypothesis.

While Cs^+ and Na^+ are both monovalent, Cs^+ should be expected to bond more strongly than Na^+ because Cs^+ has a larger ionic diameter and a lower hydration energy (Table 4). When comparing the adsorption of Cs^+ alone (Figs 2–4) to Na^+ alone on the three zeolites (Fig. 5), this pattern is confirmed. While the shapes of the adsorption envelopes for Na^+ and Cs^+ on the three zeolite minerals are very similar, the initial adsorption edge occurs at least half a pH unit lower for Cs^+ than for Na^+ on all three of the zeolites. This indicates that Cs^+ is adsorbing more strongly because a higher H^+ concentration (lower pH) is required to desorb Cs^+ than is required to desorb Na^+ from the same adsorption sites. The amount of Cs^+ adsorbed by the zeolites is also significantly larger than the amount of Na^+ adsorbed by the same zeolites, which is another indication of the much stronger affinity of these minerals for Cs^+ compared to Na^+.

Analysis of the adsorption envelopes for the three zeolites indicated that as the size of the environment in which Cs^+ is adsorbing decreases, the strength with which Cs^+ bonds to the adsorption sites in those environments increases. Zeolite Y (largest nanopores) shows the weakest Cs^+ adsorption.

Table 4. Characteristics of monovalent ions compared in this study. Ionic diameters are from Schulthess (2005) and enthalpy of hydration values were compiled by Smith (1977). A range of enthalpy of hydration values is presented to account for different methodologies for determining these values

	Ionic diameter (nm)	Hydrated diameter (nm)	Enthalpy of hydration (kJ mol^{-1})
Na^+	0.248	0.730	390–410
K^+	0.318	0.696	320–330
Cs^+	0.392	0.692	264–280

https://doi.org/10.1007/s42860-021-00150-9 Published online by Cambridge University Press

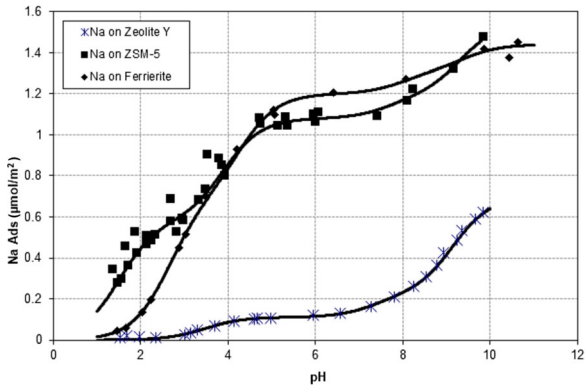

Fig. 5. Adsorption envelopes for Na^+ on zeolite Y, ZSM-5, and ferrierite. Each envelope has two distinct adsorption edges, with Na^+ showing much stronger adsorption on ZSM-5 and ferrierite than on zeolite Y (adapted from data published by Ferreira & Schulthess, 2011)

Ferrierite (smallest nanopores) shows the strongest, with ZSM-5 (medium nanopores) falling somewhere in between. The vermiculite interlayer space reduced to a distance of 0.12 nm after the adsorption of Cs^+, as evident from XRD analysis (Ferreira et al., 2018). This collapsed distance is smaller than any dimension of the nanopores for ferrierite. The adsorption of Cs^+ on vermiculite (Fig. 6) should, therefore, be more robust than on any of the zeolite minerals presented in this study. When comparing the adsorption envelopes of Cs^+ on the three zeolite minerals used in the current study (Figs 2–4) to an adsorption envelope generated for Cs^+ on vermiculite (Fig. 6), major differences are noted. The low-pH adsorption edge for Cs^+ on vermiculite occurs at ~pH 2.5, which is lower than the pH for either ZSM-5 or ferrierite. This demonstrates that Cs^+ is adsorbing more strongly on vermiculite than either of the zeolite minerals with nanopores small enough to trigger the NISE effect. One of the most remarkable differences between the adsorption of Cs^+ on vermiculite and the zeolite minerals used in this study is that even at pH 1.0, the H^+ concentration was not high enough to desorb fully 100% of the Cs^+ adsorbed in the vermiculite interlayers. In contrast, the zeolite models show that Cs^+ adsorption drops to zero at ~pH 1.5 for ZSM-5 and ~pH 1.0 for ferrierite. On vermiculite, the total amount of Cs^+ adsorbed at pH 1.0 is only 35% lower than the maximum amount of Cs^+ adsorbing at pH 7.0. This is another remarkable difference between the behavior of Cs^+ adsorbing on vermiculite compared to its adsorption in the nanopore channels of the zeolite minerals. Increasing the concentration of H^+ in solution from 10^{-7} M to 10^{-1} M causes all adsorbed Cs^+ to be desorbed in the zeolite minerals, where the Cs^+ is adsorbed quite strongly via an inner-sphere mechanism. This same change in aqueous H^+ concentration only reduces the concentration of adsorbed Cs^+ on vermiculite by a little over a third. This clearly supports the inverse relationship between the adsorption strength of Cs^+ and the size of the environment in which Cs^+ is adsorbing established by the zeolite adsorption envelopes and emphasizes why its removal from the contaminated soil in Fukushima Prefecture has proven so challenging given the tiny 0.12 nm interlayer dimension of the vermiculite clay after Cs^+ has adsorbed.

CONCLUSIONS

Adsorption envelopes showed that Cs^+ adsorbed more strongly on all three zeolite minerals than Na^+ did in previous experiments. This is probably because Cs^+ has a weaker bond to its hydrating water molecules than Na^+ and a larger ionic radius. Analysis of the adsorption envelopes for Cs^+ on the three minerals established an inverse relationship between the adsorption strength of Cs^+ and the diameter of the nanopore channels in the mineral caused by the NISE effect. The zeolite with the largest nanopores showed the weakest adsorption, and the zeolite with the smallest nanopores showed the most substantial adsorption. This pattern was further confirmed by comparing the adsorption strength of Cs^+ on these zeolite minerals to its adsorption strength on vermiculite, shown by XRD to have a collapsed interlayer dimension even smaller than the sizes of the zeolites' nanopores. The strength of the adsorption of Cs^+ on vermiculite is responsible for the difficulty in removing radiocesium from soil contaminated after the meltdown of the Fukushima Daiichi Nuclear Power Plant in Japan in 2011. In the current study, the fact that Cs^+ is

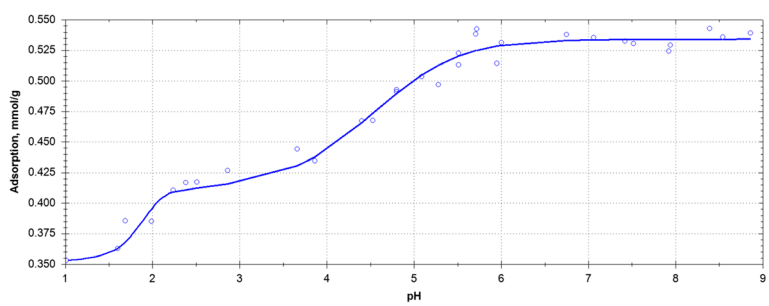

Fig. 6. Adsorption envelope for Cs^+ on vermiculite. Two adsorption edges are present, one centered at ~pH 2.5 and another centered at ~pH 5 (adapted from Ferreira et al., 2018)

https://doi.org/10.1007/s42860-021-00150-9 Published online by Cambridge University Press

adsorbing so much more strongly on vermiculite than on these zeolite minerals emphasizes how difficult the removal of that radiocesium contamination from the impacted soil is likely to be.

ACKNOWLEDGMENTS

This research project benefitted from internal funding by the College of Science and Mathematics at Kennesaw State University.

FUNDING

Funding sources are as stated in the Acknowledgments.

Declarations

Conflict of Interest

The authors declare that they have no conflict of interest.

REFERENCES

Akalin, H. A., Hiçsönmez, U., & Yilmaz, H. (2018). Removal of cesium from aqueous solution by adsorption onto Sivas-Yildizeli (Türkiye) vermiculite: Equilibrium, kinetic and thermodynamic studies. *Journal of the Turkish Chemical Society, 5*(1), 85–116.

Arai, Y., & Sparks, D. L. (2001). ATR–FTIR spectroscopic investigation on phosphate adsorption mechanisms at the ferrihydrite–water interface. *Journal of Colloid and Interface Science, 241*(2), 317–326.

Baek, W., Ha, S., Hong, S., Kim, S., & Kim, Y. (2018). Cation exchange of cesium and cation selectivity of natural zeolites: Chabazite, stilbite, and heulandite. *Microporous and Mesoporous Materials, 264*, 159–166.

Baerlocher, C. & McCusker, L.B. (2020). Database of zeolite structures. https://america.iza-structure.org/IZA-SC/ftc_table.php (accessed 23 September 2020).

Bostick, B. C., Vairavamurthy, M. A., Karthikeyan, K. G., & Chorover, J. (2002). Cesium adsorption on clay minerals: An EXAFS spectroscopic investigation. *Environmental Science and Technology, 36*, 2670–2676.

Cabrera, F., Madrid, L., & De Arambarri, P. (1977). Adsorption of phosphate by various oxides: Theoretical treatment of the adsorption envelope. *European Journal of Soil Science, 28*, 306–313.

Coleman, N. T., Craig, D., & Lewis, R. J. (1963). Ion-exchange reactions of cesium. *Soil Science Society of America Journal, 27*, 287–289.

Comans, R. N. J., & Hockley, D. E. (1992). Kinetics of cesium sorption on illite. *Geochimica et Cosmochimica Acta, 56*, 1157–1164.

Dolcater, D. L., Jackson, M. L., & Syers, J. K. (1972). Cation exchange selectivity in mica and vermiculite. *American Mineralogist, 57*, 1823–1831.

Dzene, L., Tertre, E., Hubert, F., & Ferrage, E. (2015). Nature of the sites involved in the process of cesium desorption from vermiculite. *Journal of Colloid and Interface Science, 455*, 254–260.

Ferreira, D. R., & Schulthess, C. P. (2011). The Nanopore inner-sphere enhancement (NISE) effect: Sodium, potassium, and calcium. *Soil Science Society of America Journal, 75*(2), 389–396.

Ferreira, D. R., Schulthess, C. P., & Giotto, M. V. (2012). An investigation of strong sodium retention mechanisms in nanopore environments using nuclear magnetic resonance spectroscopy. *Environmental Science and Technology, 46*, 300–306.

Ferreira, D. R., Schulthess, C. P., & Kabengi, N. J. (2013). Calorimetric evidence in support of the nanopore inner-sphere enhancement (NISE) theory on cation adsorption. *Soil Science Society of America Journal, 77*, 94–99.

Ferreira, D. R., Thornhill, J. A., Roderick, E. I. N., & Li, Y. (2018). The impact of pH and ion exchange on ^{133}Cs adsorption on vermiculite. *Journal of Environmental Quality, 47*(6), 1365–1370.

Flanagan, D.M. & Crangle Jr, R.D. (2017). Zeolites in metals and minerals: U.S. Geological Survey minerals yearbook, 1, pp. 84.1–84.4. https://www.usgs.gov/centers/nmic/minerals-yearbook-metals-and-minerals.

Fuji, K., Ikeda, S., Akama, A., Komatsu, M., Takahashi, M., & Kaneko, S. (2014). Vertical migration of radiocesium and clay mineral composition in five forest soils contaminated by the Fukushima nuclear accident. *Soil Science and Plant Nutrition, 60*, 751–764.

Fuller, A. J., Shaw, S., Ward, M. B., Haigh, S. J., Mosselmans, J. F. W., Peacock, C. L., Stackhouse, S., Dent, A. J., Trivedi, D., & Burke, I. T. (2015). Caesium incorporation and retention in illite interlayers. *Applied Clay Science, 108*, 128–134.

Gaines Jr., G. L. (1957). The ion-exchange properties of muscovite mica. *Journal of Physical Chemistry, 61*(10), 1408–1412.

Groenewold, G. S., Ingram, J. C., McLing, T., Gianotto, A. K., & Avci, R. (1998). Cs^+ speciation on soil particles by TOF-SIMS imaging. *Analytical Chemistry, 70*(3), 534–539.

Huang, X., Hu, S., Wang, F., Liu, Y., & Mu, Y. (2017). Properties of alkali-activated slag with addition of cation exchange material. *Construction and Building Materials, 146*, 321–328.

Iijima, K., Tomura, T., & Shoji, Y. (2010). Reversibility and modeling of adsorption behavior of cesium ions on colloidal montmorillonite particles. *Applied Clay Science, 49*, 262–268.

Johan, E., Yamada, T., Munthali, M. W., Kabwadza-Corner, P., Aono, H., & Matsue, N. (2015). Natural zeolites as potential materials for decontamination of radioactive cesium. *Procedia Environmental Sciences, 28*, 52–56.

Kogure, T., Morimoto, K., Tamura, K., Sato, H., & Yamagishi, A. (2012). XRD and HRTEM evidence for fixation of cesium ions in vermiculite clay. *Chemistry Letters, 41*, 380–382.

Lafferty, B. J., & Loeppert, R. H. (2005). Methyl arsenic adsorption and desorption behavior on iron oxides. *Environmental Science and Technology, 39*(7), 2120–2127.

Lee, H. A., Kim, H. S., Jeong, H. K., Park, M., Chung, D. Y., Lee, K.-Y., Lee, E. H., & Kim, W. T. (2017). Selective removal of radioactive cesium from nuclear waste by zeolites: On the origin of cesium selectivity revealed by systematic crystallographic studies. *The Journal of Physical Chemistry C, 121*(19), 10594–10608.

Lomenick, T. F., & Tamura, T. (1965). Naturally occurring fixation of cesium-137 on sediments of lacustrine origin. *Soil Science Society of America Journal, 29*(4), 383–387.

Manning, B. A., & Goldberg, S. (1996). Modeling competitive adsorption of arsenate with phosphate and molybdate on oxide minerals. *Soil Science Society Of America Journal, 60*, 121–131.

Martin, H. W., & Sparks, D. L. (1985). On the behavior of nonexchangeable potassium in soils. *Communications in Soil Science and Plant Analysis, 16*, 133–162.

McKenzie, R. M. (1983). The adsorption of molybdenum on oxide surfaces. *Australian Journal of Soil Research, 21*(4), 505–513.

Mimura, H., & Kanno, T. (1985). Distribution and fixation of cesium and strontium in zeolite A and chabazite. *Journal of Nuclear Science and Technology, 22*(4), 284–291.

Mimura, H., Tachibana, F., & Akiba, K. (1992a). Breakthrough properties of cesium in columns of ferrierites. *Journal of Nuclear Science and Technology, 29*(1), 78–85.

Mimura, H., Tachibana, F., & Akiba, K. (1992b). Ion-exchange selectivity for cesium in ferrierites. *Journal of Nuclear Science and Technology, 29*(2), 184–186.

Missana, T., Garcia-Gutierrez, M., & Alonso, U. (2004). Kinetics and irreversibility of cesium and uranium sorption onto bentonite colloids in a deep granitic environment. *Applied Clay Science, 26*, 137–150.

Okumura, M., Nakamura, H., & Machida, M. (2013). Mechanism of strong affinity of clay minerals to radioactive cesium: First-

principles calculation study for adsorption of cesium at frayed edge sites in muscovite. *Journal of the Physical Society of Japan, 82*(3), 033802–033802-5.

Osman, M. A., Caseri, W. R., & Suter, U. W. (1998). H^+/Li^+ and H^+/K^+ exchange on delaminated muscovite mica. *Journal of Colloid and Interface Science, 198*(1), 157–163.

Osman, M. A., Moor, C., Caseri, W. R., & Suter, U. W. (1999). Alkali metals ion exchange on muscovite mica. *Journal of Colloid and Interface Science, 209*(1), 232–239.

Pal, D. K., & Durge, S. L. (1989). Release and adsorption of potassium in some benchmark alluvial soils of India in relation to their mineralogy. *Pedologie, 39*(3), 235–248.

Perkins, H. F., & Tan, K. H. (1973). Potassium fixation and reconstitution of micaceous structures in soils. *Soil Science, 116*(1), 31–35.

Pulido, A., Nachtigall, P., Zukal, A., Domínguez, I., & Čejka, J. (2009). Adsorption of CO_2 on sodium-exchanged ferrierites: The bridged CO_2 complexes formed between two extraframework cations. *The Journal of Physical Chemistry C, 113*, 2928–2935.

Raven, K. P., Jain, A., & Loeppert, R. H. (1998). Arsenite and arsenate adsorption on ferrihydrite: Kinetics, equilibrium, and adsorption envelopes. *Environmental Science and Technology, 32*(3), 344–349.

Rudziński, W., Narkiewicz-Michalek, J., Szabelski, P., & Chiang, A. S. T. (1997). Adsorption of aromatics in zeolites ZSM-5: A thermodynamic-calorimetric study based on the model of adsorption on heterogeneous adsorption sites. *Langmuir, 13*, 1095–1103.

Sato, K., Fujimoto, K., Dai, W., & Hunger, M. (2013). Molecular mechanism of heavily adhesive Cs: Why radioactive Cs is not decontaminated from soil. *Journal of Physical Chemistry C, 117*(27), 14075–14080.

Sawhney, B. L. (1964). Sorption and fixation of microquantities of cesium by clay minerals: Effects of saturating cations. *Soil Science Society of America Journal, 28*(2), 183–186.

Sawhney, B. L. (1972). Selective sorption and fixation of cations by clay minerals: A review. *Clays and Clay Minerals, 20*, 93–100.

Schulthess, C. P., & Huang, C. P. (1991). Humic and fulvic acid adsorption by silicon and aluminum oxide surfaces on clay minerals. *Soil Science Society of America Journal, 55*(1), 34–42.

Schulthess, C. P. (2005). *Soil chemistry with applied mathematics*. Trafford Publ.

Schulthess, C. P., Taylor, R. W., & Ferreira, D. R. (2011). The Nanopore inner sphere enhancement effect on cation adsorption: Sodium and nickel. *Soil Science Society of America Journal, 75*(2), 378–388.

Seliman, A. (2012). Affinity and removal of radionuclides mixture from low-level liquid waste by synthetic ferrierites. *Journal of Radioanalytical and Nuclear Chemistry, 292*(2), 729–738.

Seo, S. M., Kim, H. S., Chung, D. Y., Suh, J. M., & Lim, W. T. (2014). The effect of Co^{2+}-ion exchange time into zeolite Y (FAU, Si/Al = 1.56): Their single-crystal structures. *Bulletin of the Korean Chemical Society, 35*(1), 243–249.

Sikalidis, C. A., Misaelides, P., & Alexiades, C. A. (1988). Caesium selectivity and fixation by vermiculite in the presence of various competing cations. *Environmental Pollution, 52*(1), 67–79.

Smith, D. W. (1977). Ionic hydration enthalpies. *Journal of Chemical Education, 54*(9), 540–542.

Song, W., Justice, R. E., Jones, C. A., Grassian, V. H., & Larsen, S. C. (2004). Synthesis, characterization, and adsorption properties of nanocrystalline ZSM-5. *Langmuir, 20*, 8301–8306.

Sparks, D. L. (1987). Potassium Dynamics in Soils. In B. A. Stewart (Ed.), *Advances in Soil Science* (Vol. 6, pp. 1–63). Springer.

Sparks, D. L., & Carski, T. H. (1985). Kinetics of potassium exchange in heterogeneous systems. *Applied Clay Science, 1*, 89–101.

Sparks, D. L., Zelazny, L. W., & Martens, D. C. (1980). Kinetics of potassium exchange in a Paleudult from the coastal plain of Virginia. *Soil Science Society of America Journal, 44*(1), 37–40.

Sposito, G., de Wit, J. C. M., & Neal, R. H. (1988). Selenite adsorption on alluvial soils: III. Chemical modeling. *Soil Science Society of America Journal, 52*(4), 947–950.

Tanaka, K., Takahashi, Y., Sakaguchi, A., Umeo, M., Hayakawa, S., Tanida, H., Saito, T., & Kanai, Y. (2012). Vertical profiles of iodine-131 and cesium-137 in soild in Fukushima Prefecture related to the Fukushima Daiichi nuclear power station accident. *Geochemical Journal, 46*, 73–76.

Teppen, B. J., & Miller, D. M. (2006). Hydration energy determines isovalent cation exchange selectivity by clay minerals. *Soil Science Society of America Journal, 70*(1), 31–40.

Weiss, R., & Bourgeois, J. (2012). Understanding sediments—Reducing tsunami risk. *Science, 336*(*6085*), 1117.

Yamamoto, T., Takigawa, T., Fujimura, T., Shimada, T., Ishida, T., Inoue, H., & Takagi, S. (2019). Which types of clay minerals fix cesium ions effectively? The “cavity-charge matching effect”. *Physical Chemistry Chemical Physics, 21*(18), 9352–9356.

(Received 20 January 2021; revised 3 August 2021; AE: Jocelyne Brendlé-Miehé)